Eur Biophys J (2005) 34: 19–27
DOI 10.1007/s00249-004-0428-x

ARTICLE

**Shu Zhang · Guozheng Wang · David G. Fernig
Philip S. Rudland · Stephen E. D. Webb
Roger Barraclough · Marisa Martin-Fernandez**

Interaction of metastasis-inducing S100A4 protein in vivo by fluorescence lifetime imaging microscopy

Received: 21 February 2004 / Revised: 26 May 2004 / Accepted: 27 May 2004 / Published online: 3 August 2004

Abstract Elevated levels of the calcium-binding regulatory protein, S100A4, have been shown to be causative of a metastatic phenotype in models of cancer metastasis and to be associated with reduced patient survival in breast cancer patients. Recombinant S100A4 protein interacts in vitro in a calcium-dependent manner with the heavy chain of non-muscle myosin isoform A at a protein kinase C phosphorylation site. At present, the mechanism of metastasis induction by S100A4 in vivo is almost completely unknown. The binding of S100A4 to a C-terminal recombinant fragment of non-muscle myosin heavy chain in living HeLa cells has now been shown using confocal microscopy, fluorescence lifetime imaging microscopy and time-correlated single-photon counting. The association between S100A4 and non-muscle myosin heavy chain was studied by determining fluorescence resonance energy transfer-derived changes in the fluorescence lifetime of enhanced cyan fluorescent protein fused to S100A4 in the presence of a recombinant fragment of the C-terminal region of non-muscle myosin heavy chain (rNMMHCIIA) fused to enhanced yellow fluorescent protein. There was no interaction between the non-muscle myosin heavy chain fragment and a calcium-binding-deficient mutant of S100A4 protein which has been shown to be defective in the induction of metastasis in model systems in vivo. The results demonstrate, for the first time, not only direct interaction between S100A4 and a target rNMMHCIIA in live mammalian cells, but also that the interaction between S100A4 and the non-muscle myosin heavy chain in vivo could contribute to the mechanism of metastasis induction by a high level of S100A4 protein.

Keywords Fluorescence resonance energy transfer · Non-muscle myosin · Cancer · S100A4

Abbreviations ECFP: enhanced cyan fluorescent protein · EYFP: enhanced yellow fluorescent protein · FLIM: fluorescence lifetime imaging · FRET: fluorescence resonance energy transfer · Mutant C: S100A4 protein bearing an inactivating mutant in the C-terminal EF-hand loop · PBS: phosphate-buffered saline · PCR: polymerase chain reaction · rNMMHCIIA: recombinant C-terminal fragment of non-muscle myosin heavy chain II, isoform A · TCSPC: time-correlated single-photon counting

S. Zhang · G. Wang · D. G. Fernig · P. S. Rudland
R. Barraclough (✉)
Cancer and Polio Research Fund Laboratories,
School of Biological Sciences, University of Liverpool,
Liverpool, L69 7ZB, UK
E-mail: brb@liv.ac.uk
Tel.: +44-151-7954469
Fax: +44-151-7954406

S. E. D. Webb · M. Martin-Fernandez
CLRC, Daresbury Laboratory, Daresbury,
Warrington, WA4 4AD, UK

Introduction

Ca^{2+}-binding proteins of the S100 family are low molecular weight polypeptides of between 9 and 13 kDa whose structure is characterised by four helices that form two EF-hand structures linked by a loop (Donato 1999). One S100 protein, S100A4, has been shown to cause a metastatic phenotype in rat and mouse model systems (Davies et al. 1993, 1996; Ambartsumian et al. 1996). Moreover, the presence of S100A4 in carcinoma cells is associated with metastasis or a poor prognosis in patients with carcinomas of the breast, bladder, colorectum, gall bladder, esophagus and lung (Kimura et al. 2000; Rudland et al. 2000; Ninomiya et al. 2001; Davies et al. 2002; Gongoll et al. 2002; Nakamura et al. 2002).

The mechanism by which S100A4 promotes metastasis is not well understood. The S100 proteins are thought to interact in vitro with a variety of target proteins in a calcium-dependent manner (Donato 1999), and S100A4 has been reported to interact with p53

(Grigorian et al. 2001), methionine aminopeptidase (Endo et al. 2002) and liprin β (Kriajevska et al. 2002), and with cytoskeletal proteins actin (Watanabe et al. 1993), tropomyosin (Takenaga et al. 1994b) and non-muscle myosin heavy chain (Kriajevska et al. 1994, 1998; Ford and Zain 1995; Ford et al. 1997). However, more recently, using an optical biosensor, interaction of S100A4 has been detected with p53 and with non-muscle myosin heavy chains (Chen et al. 2001, 2003). Despite all these results in vitro, there is, as yet, no direct evidence that S100A4 interacts with such targets in vivo or that the in vitro targets have any relevance for the mechanism of metastasis-induction by S100A4. In fact, the use of the yeast two-hybrid system has not identified an interaction between S100A4 and its in vitro binding partners (Tarabykina et al. 2000; Wang et al. 2000). Now, the distance-sensitive phenomenon of fluorescence resonance energy transfer (FRET) in combination with confocal imaging and fluorescence lifetime imaging microscopy (FLIM) has been used to investigate the interaction of S100A4 and non-muscle myosin in living mammalian cells.

FRET is a phenomenon by which the excited-state energy of an optically excited molecule (donor) is transferred to a neighbouring molecule (acceptor) non-radiatively via intermolecular dipole coupling (Lakowicz 1983). FRET is therefore extremely sensitive to short intermolecular distances (<10 nm), the efficiency of FRET varying as the inverse sixth power with distance (Stryer and Haugland 1967). FRET measurement of interactions between proteins inside living cells has recently become more common (reviewed in Wouters et al. 2001; Jares-Erijman and Jovin 2003). The proteins under study are typically fused to fluorescent protein tags, such as enhanced cyan fluorescent protein (ECFP) (donor) and enhanced yellow fluorescent protein (EYFP) (acceptor) (Lippincott-Schwartz and Patterson 2003). ECFP and EYFP are ideal for FRET measurement because of their excellent spectral overlap, resulting in an R_o value of $\sim$5 nm, which is the distance at which 50% of excited donor ECFP molecules will transfer energy to acceptor EYFP molecules (Tsien 1998). This large R_o value makes the ECFP/EYFP pair a good reporter of interactions between fluorescent fusion constructs. FRET results in the quenching of ECFP fluorescence and an increase in emission from EYFP, which has been detected in previous work by steady-state spectral imaging (van Kuppeveld et al. 2002; Karpova et al. 2003).

These measurements, however, are still far from routine, requiring several corrections to remove intrinsic distortions in the data, such as photobleaching, radiative transfer, and the dependence of FRET on acceptor concentration (Sekar and Periasamy 2003). More accurate distance information has been derived from the measurement of the fluorescence lifetime of the donor (Bastiaens and Squire 1999; van Kuppeveld et al. 2002), which is the average time that this molecule spends in the excited state, typically between picoseconds and a few nanoseconds (Lakowicz 1983). Competition of FRET with the fluorescence emission process shortens the fluorescence lifetime of the donor in the same distance-dependent fashion. FRET can therefore also be quantified from the measurement of the fluorescence lifetime of the donor after blocking the emission of the acceptor. Most previous measurements of the fluorescence lifetime of ECFP have been derived from measurements in the frequency domain in combination with wide-field fluorescence lifetime imaging microscopy (FLIM) (Bastiaens and Squire 1999; Pepperkok et al. 1999; Wouters et al. 2001; van Kuppeveld et al. 2002). For measurements in the frequency domain, the emitted fluorescence light is sinusoidally modulated at the same frequency as the excitation light and the average lifetime of the excited state of the ECFP molecule calculated from either the phase shift or the loss of modulation in the emitted fluorescence. The frequency method has been widely used because it does not require sub-nanosecond resolution and/or the use of expensive pulsed lasers as excitation light. However, for molecules like ECFP that have intrinsic bi-exponential fluorescence decays, different values may be derived from the shift and modulation (Pepperkok et al. 1999).

In this work we have used the novel approach of combining confocal microscopy with time-correlated single-photon counting (TCSPC) (O'Conner and Phillips 1984) to measure the fluorescence lifetime of ECFP fused to S100A4 in single living cells co-expressing a recombinant C-terminal fragment of non-muscle myosin heavy chain, isoform II (rNMMHCIIA) fused to EYFP. The use of single photons to excite fluorescence in the samples resulted in undetectable photobleaching levels in the sample while allowing rejection of out-of-focus signals ubiquitous in wide-field microscopy. TCSPC directly measures the time between the absorption and emission of individual photons, having the advantage of providing quantitative results largely free from artefacts such as photobleaching and radiative transfer (Martin-Fernandez et al. 2002). As photon absorption is near instantaneous ($\sim$1 fs), TCSPC therefore allows the accumulation of the intrinsic bi-exponential time-resolved fluorescence intensity decay of ECFP, from which its fluorescence lifetime can be unambiguously determined. The FRET data show the first direct evidence of the interaction between S100A4 and myosin in vivo and demonstrate a quick, quantitative, non-invasive assay to investigate S100A4 interactions in living cells.

Materials and methods

Plasmids and molecular biology

Living Colors plasmid vectors pEYFP and pECFP were obtained from Clontech (Palo Alto, USA). A re-

combinant fragment of non-muscle myosin II heavy chain isoform A (rNMMHCIIA) mRNA encoding the C-terminal 149 amino acids of NMMHCIIA (Chen et al. 2001, 2003) was amplified by polymerase chain reaction (PCR) using the following primers: forward 5′-CCCCAAGCTTATGCTCGAGGCCAAG-3′, reverse 5′-CGGGATCCTCTTCGGCAGGTTTG-3′ bearing *Hind*III and *Bam*HI restriction enzyme sites (underlined). Following restriction enzyme digestion, the PCR products were cloned between the *Hind*III and *Bam*HI sites of a Living Color EYFP vector such that a fusion protein was encoded consisting of EYFP attached to the C-terminus of NMMHCIIA fragment, designated NMMHCIIA-EYFP.

The mRNA for rat S100A4 was amplified by PCR using the following primers bearing *Hind*III and *Bam*HI restriction enzyme sites respectively at their 5′ ends: forward 5′-CTGTGAAGCTTCGATGGCGAGACCCTTG-3′, reverse 5′-CGGGATCCTCACTTCTTCCGGGGCTC-3′. Following restriction enzyme digestion, the PCR products were cloned between the *Hind*III and *Bam*HI sites of pECFP, such that a fusion protein was encoded consisting of the ECFP attached to the N-terminus of the S100A4, designated ECFP-S100A4.

The cDNA-encoding wild-type S100A4 protein was mutated by site-directed mutagenesis using PCR (Ho et al. 1989) so that it encoded a mutant S100A4 protein in which the C-terminal calcium-binding site was inactivated by point mutations to calcium-binding amino acids N65 to I, and D67 to A (Zhang and Barraclough, unpublished). The encoded protein in recombinant form is not only inactive in myosin binding in vitro but also fails to induce metastasis in vivo under the same conditions in which non-mutant S100A4 induces metastasis (Zhang and Barraclough, unpublished). The cDNA was amplified using the same primers described above and the resulting PCR product was digested with restriction enzymes and inserted into the pECFP vector as described above. The resulting fusion protein was designated ECFP-S100A4 mutant-C.

Production of recombinant fusion proteins in *E. coli*

The coding sequences of ECFP-S100A4, rNMMHCIIA-EYFP and EYFP were excised from the Living Color expression vectors and were inserted into an engineered pET16 vector between an *Nhe*I site (inserted adjacent to the existing *Nde*I site) and a *Bam*HI site. The open reading frames of the fusion proteins were confirmed by automated DNA sequencing (School of Biological Science, University of Liverpool). Recombinant fusion proteins and EYFP were expressed in *E. coli* strain BL 21 DE3 and purified using His.Bind Resin (Novagen, Madison, WI, USA). Polyacrylamide gel electrophoresis and Western blotting were carried out as described previously (Wang et al. 2000).

Target binding by fluorescent fusion proteins containing S100A4 and recombinant NMMHCIIA

To check that the fusion of the fluorescent proteins did not affect the ability of either S100A4 or rNMMHCIIA to interact in vitro, the interactions between the ECFP-S100A4 fusion protein and its target rNMMHCIIA, and between the rNMMHCIIA-EYFP fusion protein and S100A4 were determined using a dual-channel IAsys resonant mirror biosensor (Thermo Electron, Basingstoke, UK), as described previously (Chen et al. 2001). Prior to immobilisation on aminosilane surfaces, the purified proteins were dialysed against phosphate-buffered saline (PBS) and for the NMMHCIIA-EYFP, 0.5 M NaCl was added to the PBS. The EYFP and rNMMHCIIA-EYFP were immobilised on aminosilane surfaces using bis[sulfosuccinimidyl]suberate (Perbio, Chester, UK) as the cross-linker (Rahmoune et al. 1998a, 1998b). The soluble ligate, ECFP-S100A4, was filtered and buffer-transferred into 10 mM NaH_2PO_4, pH 7.7 using a UFV2BCC10 filter device (Millipore, Bedford, MA, USA). Binding assays consisted of adding 1 µl soluble ligate to 29 µl PBS supplemented with 0.02% (v/v) Tween-20 and 0.5 mM Ca^{2+}. The extent of binding of the ligate was calculated by fitting the data to a single-site binding model as described previously (Chen et al. 2001).

Cell culture and transfection

HeLa cervical carcinoma cells were grown in Dulbecco's modified Eagles' medium containing 10% (v/v) fetal calf serum and transferred, when they reached 80% confluence, at a split ratio of 1:5. For fluorescence lifetime imaging experiments, cells plated onto glass coverslips at a density of 50–80% were transfected with recombinant expression plasmid DNAs which had been purified using a plasmid purification kit (Qiagen, Hilden, Germany). Donor ECFP plasmids and acceptor EYFP plasmids were transfected at a ratio of 1:2 to bias the cells towards the expression of more acceptor, thereby increasing the probability of detecting FRET. Cells were used for fluorescence lifetime imaging 24–48 h after transfection.

Fluorescence lifetime imaging

Coverslips containing the transfected cells were transferred to a chamber filled with culture medium, and inserted into a purpose-built scanning confocal microscope (Van der Oord et al. 1996). Fluorescence was excited at 435 nm using a pulsed frequency-doubled Ti:sapphire laser with a repetition rate of 76 MHz (Coherent, Santa Clara, CA, USA). The light was delivered to the sample via a dichroic mirror (51017, Chroma Technology, Rockingham, VT, USA) and a 1.3-NA oil immersion objective (Carl Zeiss, Oberkochen, Germany). The fluorescence emission of ECFP

was selectively collected between 450 and 480 nm using a band-pass emission filter 51017 (Chroma Technology). The data were recorded at room temperature. FLIM images in the time domain from single cells expressing ECFP and/or EYFP fusion proteins were collected using a TCSPC FLIM module (SPC-730) (Becker & Hickl, Berlin, Germany) and a photomultiplier tube (PMH-100-1, Hamamatsu, Bridgewater, NJ, USA). The images were 256×256 pixels in size and the acquisition time was 5 min. FLIM data were analysed using SPCImage 2.0 (Becker & Hickl, Berlin, Germany) to determine the pixel distribution of the mean fluorescence lifetime of donor ECFP. A least-squares bi-exponential decay analysis ($\alpha_1\exp\{-t/\tau_1\}+\alpha_2\exp\{-t/\tau_2\}$) returns four parameters: two pre-exponential terms (α_1, α_2) and two fluorescence lifetimes (τ_1, τ_2), from which the mean fluorescence lifetime can easily be obtained using $<\tau>=(\alpha_1\tau_1+\alpha_2\tau_2)/(\alpha_1+\alpha_2)$. Only a curve-fitting analysis using two exponentials returned chi-squared (χ^2) values between 0.8 and 1.2. The values of the χ^2 were much worse when fitting the decay curves to a mono-exponential decay and were not significantly improved by using three exponentials. The FRET efficiency $E=1-(<\tau_{DA}>/<\tau_D>)$ is calculated from the mean donor fluorescence lifetimes for cells co-expressing donor and acceptor fusion proteins ($<\tau_{DA}>$) and expressing donor fusion protein only ($<\tau_D>$) (Lakowicz 1983). The distance at which protein–protein interaction occurs can be estimated by applying $R=R_o[E^{-1}-1^{1/6}]$, where R_o (Förster radius or distance at which 50% of the donor molecules transfer energy to acceptor) is 5 nm for the ECFP/EYFP pair.

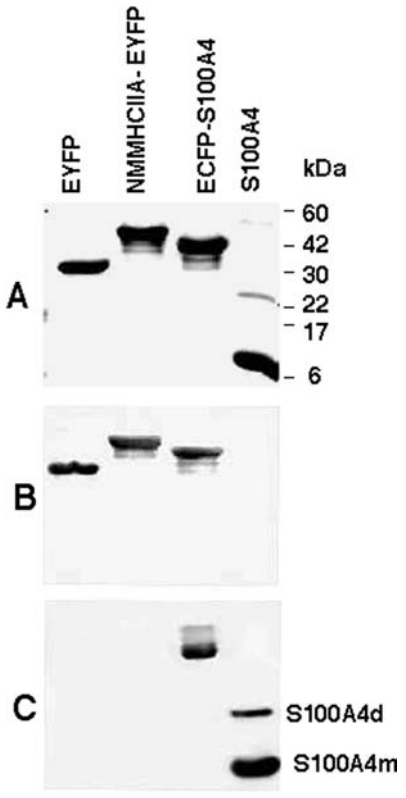

Fig. 1A–C Expression of recombinant fluorescent fusion proteins in *E. coli* cells. **A** Ten micrograms of enhanced yellow fluorescent protein (*EYFP*), *NMMHCIIA-EYFP* fusion protein, enhanced cyan fluorescent protein (*ECFP*)-*S100A4* fusion protein and *S100A4* protein with no fluorescent tag were purified from bacterial cultures as described in Materials and methods, subjected to polyacrylamide gel electrophoresis and the gel was stained with Coomassie blue. Duplicate gels (5 μg protein in each lane) were blotted onto PVDF membranes and probed with antibodies to green fluorescent protein (**B**) or to S100A4 (**C**). *S100A4m* indicates the monomer band and *S100A4d* indicates the SDS-resistant dimer band

Results and discussion

Production and characterisation of recombinant fluorescence fusion proteins

Recombinant fusion proteins expressed in *E. coli* were purified using histidine tags and their purity examined by polyacrylamide gel electrophoresis. Their identities were confirmed by Western blotting with green fluorescent protein and S100A4 antibodies (Fig. 1). The his-tagged EYFP, EYFP-rNMMHCIIA and ECFP-S100A4 migrated at molecular weights of 29, 50 and 41 kDa respectively (Fig. 1).

An optical biosensor was used to find out the extent to which the fluorescent protein tags on the S100A4 and rNMMHCIIA molecules affected the previously described interaction in vitro between S100A4 and rNMMHCIIA (Kriajevska et al. 1994; Ford and Zain 1995; Chen et al. 2001, 2003). Rat S100A4 was shown to interact with NMMHCIIA-EYFP immobilised on a biosensor surface. The extent of interaction was reduced by about 25% when the ECFP-S100A4 fusion protein was used (Fig. 2). Thus, the presence of the fluorescent protein tag affected only marginally the ability of the S100A4 protein to interact with rNMMHCIIA. There was virtually undetectable interaction between S100A4 or ECFP-S100A4 and immobilised EYFP (Fig. 2), indicating that any observed interaction occurred with the rNMMHCIIA component of the fusion protein.

Fluorescence resonance energy transfer between ECFP-S100A4 and rNMMHCIIA-EYFP by fluorescence lifetime imaging

Cover slips bearing cells that had been (co)transfected with cDNAs encoding ECFP and/or EYFP fusion proteins were placed on the sample stage of a scanning confocal microscope. All samples were illuminated with pulsed light at 435 nm, which is the optimal wavelength for ECFP excitation. The fluorescence emission from ECFP was then selectively recorded through an interference filter, as described in Materials and methods. To investigate whether unwanted fluorescence photons from EYFP could still reach the detector, FLIM images

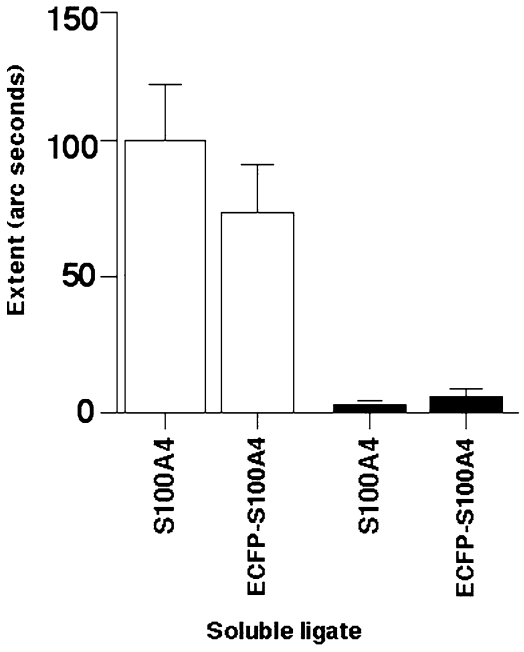

Fig. 2 Interactions of fluorescent fusion proteins using an optical biosensor. rNMMHCIIA-EYFP (*white columns*) or EYFP (*black columns*) was immobilised on an aminosilane surface, and the extent of binding of ligates, rat *S100A4* or *ECFP-S100A4* fusion protein, was measured using an optical biosensor, as described in Materials and methods. The results are expressed as mean ± SD from at least three independent binding assays for each pair of proteins

were first recorded from three samples of cells transfected only with acceptor fusion protein rNMMHCIIA-EYFP and no ECFP. No significant signal above the noise level of the detector was discernible (data not shown), showing that fluorescence photons from EYFP were effectively eliminated by the filter employed and did not reach the detector. The data also showed that the contribution from cell autofluorescence was negligible.

Scanning confocal images (Fig. 3) show examples of the intensity distribution of the fluorescence from ECFP-S100A4 recorded in two HeLa cells, one co-transfected with donor ECFP-S100A4 and acceptor rNMMHCIIA-EYFP (Fig. 3A), and the second transfected with ECFP-S100A4 alone (Fig. 3B). An optical section through the cell nucleus showed the ECFP-S100A4 preferentially localised in the cytosol (Fig. 3A). The image in Fig. 3B was recorded from an optical section closer to the top surface of the cell. Figure 3C shows two typical time-resolved fluorescence decays corresponding to the pixels marked by arrows in Fig. 3A (solid circles) and B (open circles). The fluorescence decays show two rates of depopulation of the excited state of ECFP. The fluorescence decays were least squares fitted to the bi-exponential equation (Fig. 3C, D) and the mean fluorescence lifetime of ECFP was calculated for each pixel, as described above. The resulting FLIM maps (Fig. 4A, B; left) show the distribution across the cells of the mean fluorescence lifetime of ECFP. The histograms on the right show the time

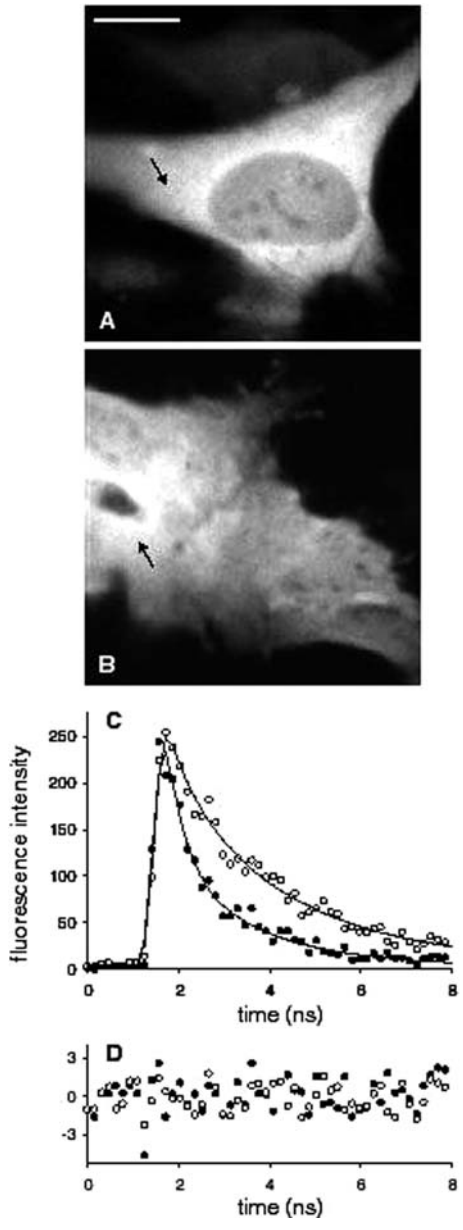

Fig. 3A–D Confocal imaging of HeLa cells transfected with ECFP and EYFP constructs. **A** Confocal microscopy intensity image showing the intracellular distribution of ECFP-S100A4 in a living HeLa cell co-expressing ECFP-S100A4 and rNMMHCIIA-EYFP. The *bar* is 20 μm. **B** as **A** but recorded from a cell expressing ECFP-S100A4 alone. **C** Time-resolved fluorescence lifetime decays of the fluorescence intensity of ECFP corresponding to the pixels marked by the *arrows* in **A** (*filled circles*) and **B** (*empty circles*). The time per channel is 0.157 ns. Time courses were fitted to the bi-exponential equation for decay. The fit, shown by the *curved lines* in **C**, returned the residuals (i.e. data minus fit) shown in **D**

distribution of the fluorescence lifetimes in the two FLIM images; their widths reflect the degree of heterogeneity of the donor ECFP fluorescence lifetime. In these two examples the fluorescence lifetime distributions display maxima at 1.32 ns (Fig. 4A) and 2.55 ns (Fig. 4B). The longer value for the fluorescence lifetime of ECFP (Fig. 4B) is consistent with the unquenched

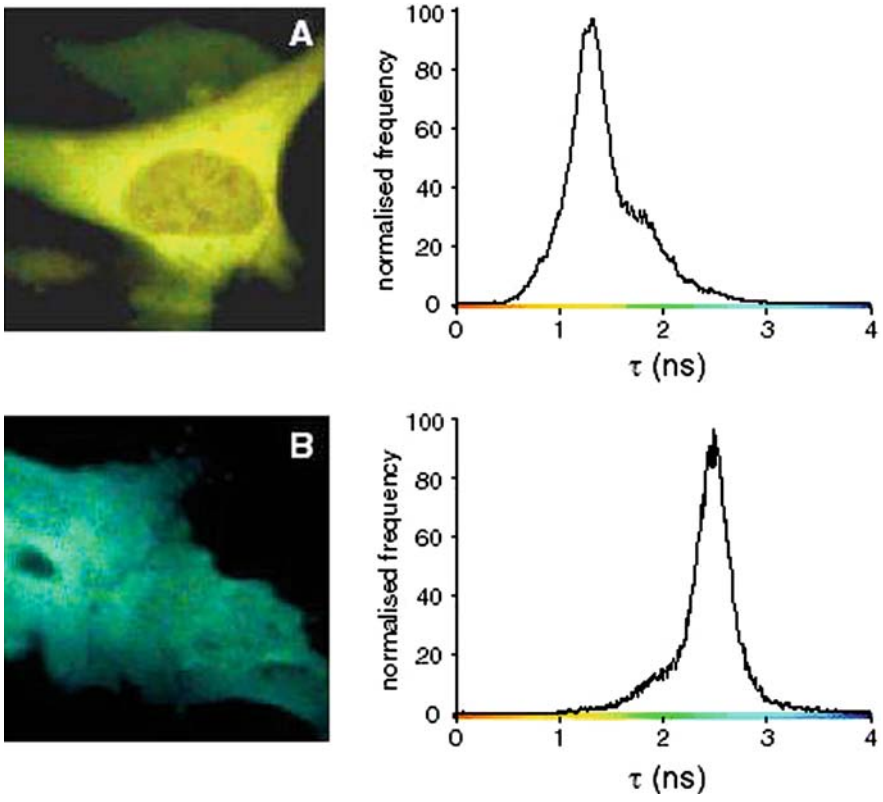

Fig. 4A, B FLIM analysis for ECFP in living HeLa cells. The HeLa cells shown in Fig. 3, co-expressing wild type S100A4-ECFP and rNMMHCIIA-EYFP fusion protein (**A**) or expressing S100A4-ECFP alone (**B**) are imaged pseudocoloured according to the fluorescence lifetime scale of the *x-axes* of the graphs. The graphs show the corresponding normalised distributions of the mean fluorescence lifetimes (τ) of ECFP

value previously measured by others from ECFP fusion constructs in the absence of acceptor (Pepperkok et al. 1999; van Kuppeveld et al. 2002). The shorter fluorescence lifetimes were recorded in the presence of acceptor (Fig. 4A), suggesting the occurrence of FRET, and therefore interaction in vivo between S100A4 and rNMMHCIIA. FRET was detected predominantly in the cytoplasm of the cells, suggesting that there was interaction between newly synthesised molecules of S100A4 and rNMMHCIIA.

However, to correlate unequivocally the shortening of the lifetime with FRET, other factors that could result in the shortening of the fluorescence lifetime of ECFP, such as changes in the environment around the proteins expressed from the transfected expression plasmids, protein overexpression, and/or fortuitous binding among the fluorescence proteins (Griesbeck et al. 2001), needed to be eliminated. To this end, we collected FLIM images from 58 individual HeLa cells in 20 transfected samples. Cells were (co)transfected with either (1) ECFP-S100A4 and rNMMHCIIA-EYFP, (2) ECFP alone, (3) ECFP and EYFP, (4) ECFP-S100A4 alone, (5) ECFP-S100A4 and EYFP, (6) ECFP-S100A4 mutant C (an inactive calcium and rNMMHCIIA-binding defective mutant of S100A4) and rNMMHCIIA-EYFP, or (7) ECFP-S100A4 and S100A4-YFP. Experiments 2, 3, 4, 5 and 6 were used as negative controls to investigate the magnitude of the changes in the fluorescence lifetime of ECFP to be expected from environmental effects, overexpression, and/or fortuitous binding to EYFP. The negative control result of 5, ECFP-S100A4 and EYFP, confirms the virtually undetectable interaction observed between these purified proteins in the biosensor experiments. FLIM data from cells co-transfected with ECFP-S100A4 and S100A4-EYFP (7) were used as a positive control, because S100A4 is known to form homodimers in the yeast two-hybrid system (Tarabykina et al. 2001).

Figure 5A shows the distributions of the mean fluorescence lifetimes of ECFP from 15 cells in 5 cultures co-transfected with donor ECFP-S100A4 and acceptor rNMMHCIIA-EYFP. Most (13/15) of these distributions displayed maxima at values below 2 ns, which is significantly shorter than the mean fluorescence lifetime, 2.5–3 ns, of ECFP-S100A4 when the acceptor is not present (Pepperkok et al. 1999; Tramier et al. 2002; van Kuppeveld et al. 2002). Two cells, however, showed lifetimes of about 2.7 ns. The observation that not all cells exhibit a shortened ECFP fluorescence lifetime in the presence of acceptor has been reported previously to be due to cell-to-cell heterogeneity (van Kuppeveld et al. 2002), showing the importance of recording FLIM data at the single-cell level. The fluorescence lifetime distributions from cells expressing the ECFP vector alone (blue traces, Fig. 5B), and cells co-expressing both ECFP and EYFP (black traces, Fig. 5B), both show the longer values typical of the unquenched fluorescence lifetime of ECFP, all maxima in these distributions displaying values above 2 ns. This was also the case for the distributions from cells co-expressing ECFP-S100A4 and EYFP (blue traces, Fig. 5C), and from cells

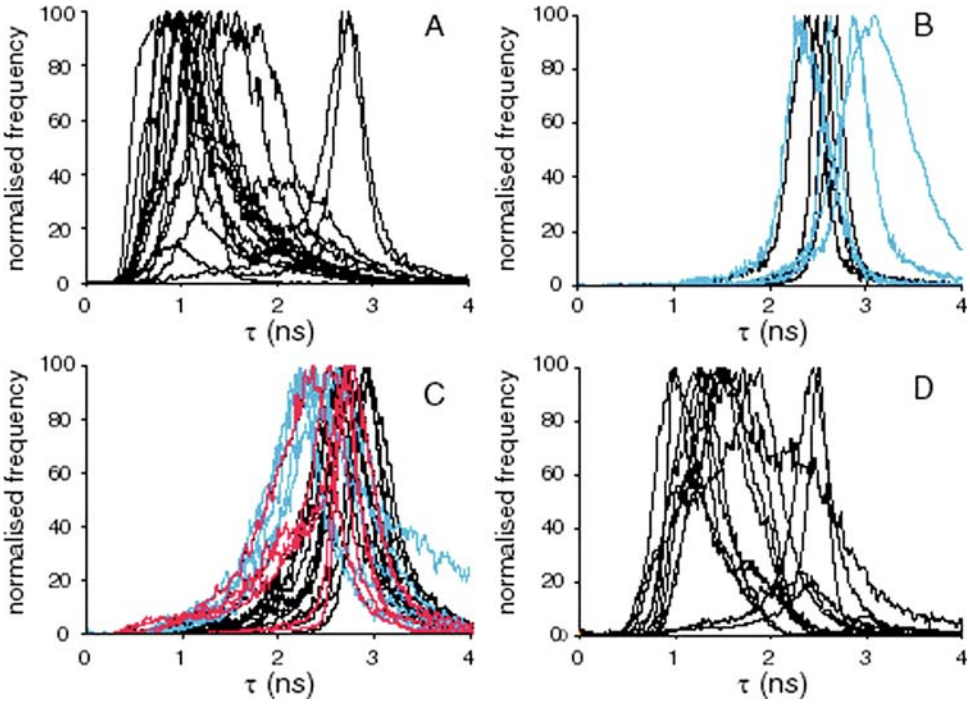

Fig. 5A–D Fluorescence lifetime histograms for ECFP across the FLIM images of individual cells. **A** Cells co-transfected with ECFP-S100A4 and rNMMHCIIA-EYFP. **B** Control cells transfected with ECFP only (*black traces*) or co-transfected with ECFP and EYFP (*blue traces*). **C** Cells transfected with ECFP-S100A4 only (*black traces*), or cells co-transfected with ECFP-S100A4 and EYFP (*blue traces*), or cells co-transfected with S100A4-mutant C and rNMMHCIIA-EYFP (*red traces*). **D** Cells co-transfected with ECFP-S100A4 and S100A4-EYFP

expressing ECFP-S100A4 alone (black traces, Fig. 5C). These results strongly suggest that neither environmental factors, nor overexpression of S100A4 by itself, nor any fortuitous binding between the fusion proteins can account for the magnitude of the shortening found in the fluorescence lifetime of ECFP in cells co-expressing ECFP-S100A4 and rNMMHCIIA-EYFP (Fig. 5A).

The mutant S100A4 protein, mutant C, does not interact at all with the rNMMHCIIA in vitro using gel overlay or an optical biosensor (Zhang and Barraclough, submitted) despite being at least 98% identical to non-mutant S100A4. The fact that there is no shortening of the fluorescence lifetime with the S100A4 mutant C (Fig. 5C, red traces) makes it very unlikely that the lifetime shortening observed with the wild-type S100A4 arises from non-specific interaction between S100A4 and rNMMHCIIA caused by locally high levels of the proteins resulting from the expression of transfected genes. Since the mutant-C protein is defective in calcium binding (Zhang and Barraclough, submitted), its failure to interact with rNMMHCIIA suggests calcium-dependence of the interaction detected by FRET.

Evidence of appreciable fluorescence lifetime shortening was found for the positive control, i.e. in the majority of cells (10/12) co-expressing homodimeric ECFP-S100A4 and S100A4-EYFP (Fig. 5D). The observed mean fluorescence lifetime of ECFP-S100A4 in the presence of rNMMHCIIA-EYFP is significantly shorter than that of the controls (Student's paired *t*-test, $P \leq 0.003$), as is the case for homodimerisation of ECFP-S00A4 and S100A4-EYFP (Student's *t*-test, $P = 0.023$) (Table 1).

Taken together these data provide strong evidence for the occurrence of FRET arising from the direct interaction between wild-type S100A4 and recombinant rNMMHCIIA in living HeLa cells. The C-terminal region of rNMMHCIIA was shown previously to self-associate (Kriajevska et al. 1998, 2000; Murakami et al. 2000) and to bind S100A4 in vitro (Kriajevska et al. 1998) as do intact non-muscle myosin heavy chains (Kriajevska et al. 1994; Ford and Zain 1995; Ford et al.

Table 1 Mean fluorescence lifetimes of donor-enhanced cyan fluorescent protein[a] returned by the fluorescence lifetime imaging analysis

Donor construct	Acceptor construct	$\tau \pm$SD (ns)
ECFP-S100A4	rNMMHCIIA-EYFP	1.31 ± 0.59[b]
ECFP	None	2.56 ± 0.10
ECFP	EYFP	2.73 ± 0.35
ECFP-S100A4	None	2.70 ± 0.16
ECFP-S100A4	EYFP	2.38 ± 0.15
ECFP-S100A4 mutant C	rNMMHCIIA-EYFP	2.6 ± 0.16
ECFP-S100A4	S100A4-EYFP	1.58 ± 0.48[c]

[a]HeLa cells were transfected with enhanced cyan fluorescent protein (*ECFP*) donor constructs and enhanced yellow fluorescent protein (*EYFP*) acceptor constructs as indicated

[b]Statistically significantly different (Student's paired *t*-test) from cells transfected with: ECFP alone ($P = 0.001$), ECFP and EYFP ($P = 0.003$), ECFP-S100A4 alone ($P = 0.0001$), ECFP-S100A4 and EYFP ($P = 0.001$), and ECFP-S100A4-mutant C and rNMMHCIIA-EYFP ($P = 0.0001$). Not statistically significantly different from cells transfected with ECFP-S100A4 and EYFP-S100A4 ($P = 0.221$)

[c]Statistically significantly different (Student's paired *t*-test) from cells transfected with: ECFP only ($P = 0.009$), ECFP and EYFP ($P = 0.023$), ECFP-S100A4 alone ($P = 0.001$), and ECFP-S100A4 and EYFP ($P = 0.004$). Not statistically significantly different from cells transfected with ECFP-S100A4 and rNMMHCIIA-EYFP ($P = 0.221$)

1997). Thus, the interaction detected by FRET between S100A4 and the C-terminal fragment of non-muscle myosin heavy chain is likely to be similar to the interaction of S100A4 with intact NMMHCIIA molecules.

Interestingly, the standard deviations in Table 1 show a larger degree of heterogeneity in the magnitude of the FRET-derived donor ECFP fluorescence lifetimes across the images of cells co-expressing donor ECFP-S100A4 and acceptor rNMMHCIIA-EYFP than in cells expressing either only donor, or donor and the empty EYFP vector. The degree of heterogeneity in cells co-expressing ECFP-S100A4 and S100A4-EYFP was also larger. Heterogeneity in cells expressing donor and acceptor S100A4 can be explained by the ability of S100A4 to dimerise, as cells will display different proportions of dimers containing donor/donor and donor/acceptor. The more frequent occurrence in a cell of donor/donor pairs will result in its fluorescence lifetime distribution peaking at longer fluorescence lifetime values. A further degree of cell-derived heterogeneity would also be expected if the S100A4 molecule were able to form multimers as well as dimers (Zacharias et al. 2002). The degree of heterogeneity in cells co-expressing ECFP-S100A4 and S100A4-EYFP is very similar to that found in cells co-expressing ECFP-S100A4 and rNMMHCIIA-EYFP (Table 1). These results suggest that, in cells co-expressing ECFP-S100A4 and rNMMHCIIA-EYFP, the observed heterogeneity may also be due to the presence of a variable population of dimerised/multimerised ECFP-S100A4, which would result in different degrees of FRET for each cell. We cannot infer from these data whether ECFP-S100A4 dimers/multimers as well as monomers are able to bind rNMMHCIIA-ECFP. We are currently carrying out these investigations.

The results are the first report of interaction in vivo between the metastasis-associated protein, S100A4 and one of its potential targets described previously in vitro (Kriajevska et al. 1994; Ford and Zain 1995) and suggest strongly that S100A4 acts, at least in part, by an interaction in vivo with rNMMHCIIA. The fact that a mutant S100A4 protein which fails to induce metastasis in an in vivo model system also fails to interact with the rNMMHCIIA in vivo using the FRET techniques, opens the possibility that the interaction of S100A4 shown in the present paper could be involved in the induction of a metastatic phenotype in vivo.

Acknowledgements This work was supported by the North West Cancer Research Fund and the Cancer and Polio Research Fund.

References

Ambartsumian N, Grigorian M, Larsen F, Karlstrom O, Sidenius N, Rygaard J, Georgiev G, Lukanidin E (1996) Metastasis of mammary carcinomas in GRS/A hybrid mice transgenic for the *mts*1 gene. Oncogene 13:1621–1630

Bastiaens P, Squire A (1999) Fluorescence lifetime imaging microscopy: spatial resolution of biochemical processes in the cell. Trends Cell Biol 9:48–52

Chen H-L, Fernig DG, Rudland PS, Sparks A, Wilkinson MC, Barraclough R (2001) Binding to intracellular targets of the metastasis-inducing protein, S100A4 (p9Ka). Biochem Biophys Res Commun 286:1212–1217

Chen H-L, Fernig DG, Rudland PS, Sparks A, Wilkinson MC, Barraclough R (2003) Binding to intracellular targets of the metastasis-inducing protein, S100A4 (p9Ka). Biochem Biophys Res Commun 308:408

Davies BR, Davies MPA, Gibbs FEM, Barraclough R, Rudland PS (1993) Induction of the metastatic phenotype by transfection of a benign rat mammary epithelial cell line with the gene for p9Ka, a rat calcium-binding protein but not with the oncogene EJ ras-1. Oncogene 8:999–1008

Davies MPA, Rudland PS, Robertson L, Parry EW, Jolicoeur PS, Barraclough R (1996) Expression of the calcium-binding protein S100A4 (p9Ka) in MMTV-neu transgenic mice induces metastasis of mammary tumours. Oncogene 13:1631–1637

Davies BR, O'Donnell M, Durkan GC, Rudland PS, Barraclough R, Neal DE, Mellon JK (2002) Expression of S100A4 protein is associated with metastasis and reduced survival in human bladder cancer. J Pathol 196:292–299

Donato R (1999) Functional roles of S100 proteins, calcium-binding proteins of the EF-hand type. Biochim Biophys Acta 1450:191–231

Endo H, Takenaga K, Kanno T, Satoh H, Mori S (2002) Methionine aminopeptidase 2 is a new target for the metastasis-associated protein, S100A4. J Biol Chem 277:26396–26402

Ford H, Zain S (1995) Interaction of metastasis associated Mts1 protein with non-muscle myosin. Oncogene 10:1597–1605

Ford H, Salim M, Chakravarty R, Aluiddin V, Zain S (1995) Expression of Mts1, a metastasis-associated gene, increases motility but not invasion of a non-metastatic mouse mammary adenocarcinoma cell line. Oncogene 11:2067–2075

Ford H, Silver D, Cachar B, Sellers J, Zain S (1997) Effect of Mts1 on the structure and activity of nonmuscle myosin II. Biochemistry 36:16321–16327

Gongoll S, Peters G, Mengel M, Piso P, Klempnauer J, Kreipe H, von Wasielewski R (2002) Prognostic significance of calcium-binding protein S100A4 in colorectal cancer. Gastroenterology 123:1478–1484

Griesbeck O, Baird GS, Campbell RE, Zacharias DA, Tsien RY (2001) Reducing the environmental sensitivity of yellow fluorescent protein. Mechanism and applications. J Biol Chem 276:29188–29194

Grigorian M, Andresen S, Tulchinsky E, Kriajevska M, Carlberg C, Kruse C, Cohn M, Ambartsumian N, Christensen A, Selivanova G, Lukanidin E (2001) Tumor suppressor p53 protein is a new target for the metastasis-associated Mts1/S100A4 protein: functional consequences of their interaction. J Biol Chem 276:22699–22708

Ho S, Hunt H, Horton R, Pullen J, Pease L (1989) Site-directed mutagenesis by overlap extension using the polymerase chain-reaction. Gene 77:51-59

Jares-Erijman E, Jovin T (2003) FRET imaging. Nat Biotechnol 21:1387–1395

Jenkinson SR, Barraclough R, West CR, Rudland PS (2004) S100A4 regulates cell motility and invasion in an in vitro model for breast cancer metastasis. Br J Cancer 90:253–262

Karpova T, Baumann C, He L, Wu X, Grammer A, Lipsky P, Hager G, McNally J (2003) Fluorescence resonance energy transfer from cyan to yellow fluorescence protein detected by acceptor photobleaching using confocal microscopy and a single laser. J Microsc 209:56–70

Kimura K, Endo Y, Yonemura Y, Heizmann C, Schäfer B, Watanabe Y, Sasaki T (2000) Clinical significance of S100A4 and E-cadherin-related adhesion molecules in non-small cell lung cancer. Int J Oncol 16:1125–1131

Kriajevska M, Cardenas M, Grigorian M, Ambartsumian N, Georgiev G, Lukanidin E (1994) Non-muscle myosin heavy chain as a possible target for protein encoded by metastasis-related *mts*-1 gene. J Biol Chem 269:19679–19682

Kriajevska M, Tarabykina S, Bronstein I, Maitland N, Lomonosov M, Hansen K, Georgiev G, Lukanidin E (1998) Metastasis-associated Mts1 (S100A4) protein modulates protein kinase C phosphorylation of the heavy chain of nonmuscle myosin. J Biol Chem 273:9852–9856

Kriajevska M, Bronstein IB, Scott DJ, Tarabykina S, Fischer-Larsen M, Issinger O, Lukanidin E (2000) Metastasis-associated protein Mts1 (S100A4) inhibits CK2-mediated phosphorylation and self-assembly of the heavy chain of non-muscle myosin. Biochim Biophys Acta 1498:252–263

Kriajevska M, Fischer-Larsen M, Moertz E, Vorm O, Tulchinsky E, Grigorian M, Ambartsumian N, Lukanidin E (2002) Liprin beta 1, a member of the family of LAR transmembrane tyrosine phosphatase-interacting proteins, is a new target for the metastasis-associated protein S100A4 (Mts1). J Biol Chem 277:5229–5235

Lakowicz J (1983) Principles of fluorescence spectroscopy. Plenum, New York

Lippincott-Schwartz J, Patterson GH (2003) Development and use of fluorescent protein markers in living cells. Science 300:87–91

Martin-Fernandez M, Clarke D, Tobin M, Jones S, Jones G (2002) Preformed oligomeric epidermal growth factor receptors undergo an ectodomain change during signalling. Biophys J 82:2415–2427

Murakami N, Kotula L, Hwang Y (2000) Two distinct mechanisms for regulation of nonmuscle myosin assembly via the heavy chain: phosphorylation for MIIB and mts 1 binding for MIIA. Biochemistry 39:11441–11451

Nakamura T, Ajiki T, Murao S, Kamigaki T, Maeda S, Ku Y, Kuroda Y (2002) Prognostic significance of S100A4 expression in gallbladder cancer. Int J Oncol 20:937–41

Ninomiya I, Ohta T, Fushida S, Endo Y, Hashimoto T, Yagi M, Fujimura T, Nishimura G, Tani T, Shimizu K, Yonemura Y, Heizmann CW, Schäfer B, Sasaki T, Miwa K (2001) Increased expression of S100A4 and its prognostic significance in esophageal squamous cell carcinoma. Int J Oncol 18:715–720

O'Conner D, Phillips D (1984) Time-correlated single photon counting. Academic Press, New York.

Pepperkok R, Squire A, Geley S, Bastiaens PI (1999) Simultaneous detection of multiple green fluorescent proteins in live cells by fluorescence lifetime imaging microscopy. Curr Biol 9:269–272

Rahmoune H, Chen HL, Gallagher JT, Rudland PS, Fernig DG (1998a) Interaction of heparan sulfate from mammary cells with acidic fibroblast growth factor (FGF) and basic FGF—regulation of the activity of basic FGF by high and low affinity binding sites in heparan sulfate. J Biol Chem 273:7303–7310

Rahmoune H, Rudland PS, Gallagher JT, Fernig DG (1998b) Hepatocyte growth factor scatter factor has distinct classes of binding site in heparan sulfate from mammary cells. Biochemistry 37:6003–6008

Rudland PS, Platt-Higgins A, Renshaw C, West CR, Winstanley JHR, Robertson L, Barraclough R (2000) Prognostic significance of the metastasis-inducing protein S100A4 (p9Ka) in human breast cancer. Cancer Res 60:1595–1603

Sekar R, Periasamy A (2003) Fluorescence resonance energy transfer (FRET) microscopy imaging of live cell protein localizations. J Cell Biol 160:629–633

Stryer L, Haugland R (1967) Energy transfer: a spectroscopic ruler. Proc Natl Acad Sci USA 58:719–726

Takenaga K, Nakamura Y, Endo H, Sakiyama S (1994a) Involvement of S100-related calcium-binding protein pEL98 (or mts1) in cell motility and tumour cell invasion. Jpn J Cancer Res 85:831–839

Takenaga K, Nakamura Y, Sakiyama S, Hasegawa Y, Sato K, Endo H (1994b) Binding of pEL98 protein, an S100-related calcium-binding protein, to non-muscle tropomyosin. J Cell Biol 124:757–768

Tarabykina S, Kriajevska M, Scott DJ, Hill TJ, Lafitte D, Derrick PJ, Dodson GG, Lukanidin E, Bronstein I (2000) Heterocomplex formation between metastasis-related protein S100A4 (Mts1) and S100A1 as revealed by the yeast two-hybrid system. FEBS Lett 475:187–191

Tarabykina S, Scott DJ, Herzyk P, Hill TJ, Tame JR, Kriajevska M, Lafitte D, Derrick PJ, Dodson GG, Maitland NJ, Lukanidin EM, Bronstein IB (2001) The dimerization interface of the metastasis-associated protein S100A4 (Mts1): in vivo and in vitro studies. J Biol Chem 276:24212–24222

Tramier M, Gautier I, Piolot T, Ravaler S, Kemnitz K, Coppey J, Durieux C, Mignotte V, Coppey-Moisan M (2002) Picosecond-hetero-FRET microscopy to probe protein-protein interactions in live cells. Biophys J 83:3570–3577

Tsien RY (1998) The green fluorescent protein. Annu Rev Biochem 67:509–544

Van der Oord C, Jones G, Shaw D, Munro I, Levine Y, Gerritsen H (1996) High resolution confocal microscopy using synchrotron radiation. J Microsc 182:217–224

van Kuppeveld FJ, Melchers WJ, Willems PH, Gadella TW Jr (2002) Homomultimerization of the coxsackievirus 2B protein in living cells visualized by fluorescence resonance energy transfer microscopy. J Virol 76:9446–9456

Wang G, Rudland PS, White MRH, Barraclough R (2000) Interaction in vivo and in vitro of the metastasis-inducing S100 protein S100A4 (p9Ka) with S100A1. J Biol Chem 275:11141–11146

Watanabe Y, Usada N, Minami H, Morita T, Tsugane S-i, Ishikawa R, Kohama K, Tomida Y, Hidaka H (1993) Calvasculin as a factor affecting the microfilament assemblies in rat fibroblasts transfected by *src* gene. FEBS Lett 324:51–55

Wouters F, Verveer P, Bastiaens P (2001) Imaging biochemistry inside cells. Trends Cell Biol 11:203–211

Zacharias D, Violin J, Newton AC, Tsien R (2002) Partitioning of lipid-modified GFPs into membrane microdomains of live cells. Science 296:913–916